

INDENTATION PROTOCOL TO DETERMINE VISCOELASTIC  
PROPERTIES OF CARTILAGE BEFORE AND AFTER CROSSLINKING

A Thesis

Submitted to the Faculty

of

Purdue University

by

Shaunak A. Chandwadkar

In Partial Fulfillment of the

Requirements for the Degree

of

Master of Science in Mechanical Engineering

December 2017

Purdue University

Indianapolis, Indiana

**THE PURDUE UNIVERSITY GRADUATE SCHOOL**  
**STATEMENT OF COMMITTEE APPROVAL**

Dr. Diane Wagner, Chair

Department of Mechanical Engineering

Dr. Alan Jones

Department of Mechanical Engineering

Dr. Jong Ryu

Department of Mechanical Engineering

**Approved by:**

Dr. Sohel Anwar

Chair of the Graduate Program

Dedicated to my family and especially to my parents, Anant and Asawari, my brother Shashwat, and my grandparents Madhukar and Nalini. I feel blessed to have them as my family.

## ACKNOWLEDGMENTS

I would like to express my sincere gratitude to my advisor, Dr. Diane Wagner, for her guidance and motivation throughout my research. Working under her direction had helped me grow professionally and personally. I learned invaluable lessons from her, which will be helping me for rest of my life. I also want to thank my thesis committee members, Dr. Alan Jones and Dr. Jong Ryu for their invaluable suggestions to improve my research.

I would like to thanks my parents, Anant and Asawari Chandwadkar for their unconditional support in all walks of my life. I thank my brother, Shashwat Chandwadkar for his loving support during my research journey.

Finally, I want to thank my laboratory fellows, Huseyin Arman, Jayed Hossain, Amin Joukar, Dr. Nizeet Izath Aguilar, Dr. David Kahn and Ghazal Hosseini for their help during my research. A special thanks to all my friends who made my research journey easier with their support.

## TABLE OF CONTENTS

	Page
LIST OF TABLES . . . . .	vii
LIST OF FIGURES . . . . .	viii
SYMBOLS . . . . .	x
ABBREVIATIONS . . . . .	xi
ABSTRACT . . . . .	xii
1 BACKGROUND . . . . .	1
1.1 Cartilage Structure and Composition . . . . .	2
1.2 Cartilage Disease . . . . .	4
1.2.1 Osteoarthritis, OA . . . . .	4
1.2.2 Post-Traumatic Osteoarthritis, PTOA . . . . .	4
1.3 Cartilage Crosslinking . . . . .	5
1.3.1 Photo-Chemical Crosslinking . . . . .	5
1.4 Cartilage Indentation . . . . .	6
2 INDENTATION PROTOCOL . . . . .	7
2.1 Standard Linear Solid Model of Indentation . . . . .	8
2.2 Repeatability . . . . .	10
2.2.1 Ensuring Sample Repositionability . . . . .	10
2.2.2 Actuator Calibration Protocol . . . . .	12
2.2.3 Indentation Data Interpretation . . . . .	13
2.2.4 Indenter Size Optimization . . . . .	18
2.2.5 Indentation Depth Optimization . . . . .	20
2.2.6 Cartilage Degradation and Arbitrary Error . . . . .	22
2.2.7 Verification of Repeatability . . . . .	24
2.3 Summary . . . . .	26

	Page
3 PHOTO-CHEMICAL CROSSLINKING . . . . .	27
3.1 Crosslinking Protocol . . . . .	27
3.1.1 Method . . . . .	27
3.1.2 Laser Output Issue . . . . .	29
3.1.3 Stiffness Loss in Cartilage After Crosslinking . . . . .	31
3.1.4 Indentation . . . . .	33
3.1.5 Effect of Photo-Chemical Crosslinking . . . . .	33
3.1.6 Laser Time Optimization . . . . .	36
3.2 Discussion . . . . .	37
4 FUTURE DIRECTIONS . . . . .	39
4.1 Investigating Methods to Diffuse CASPc From Cartilage Tissue . . . . .	39
4.2 Optimize the Indentation Protocol . . . . .	39
4.3 Detecting Crosslinks Through Alternative Mechanical Testing Methods . . . . .	40
REFERENCES . . . . .	41

## LIST OF TABLES

Table	Page
2.1 Indentation test parameters . . . . .	26
2.2 Untreated cartilage properties . . . . .	26

## LIST OF FIGURES

Figure	Page
1.1 Cartilage zones . . . . .	3
2.1 Standard linear solid (SLS) model . . . . .	8
2.2 Superglued cartilage specimen . . . . .	11
2.3 Machined grooves on base plate . . . . .	11
2.4 Recalibration test, (a) shows the needle punching hole in a paper sheet (b) shows the needle entering the previously punched hole in paper after the machine was shut off and re-calibrated. . . . .	13
2.5 Load and displacement versus time obtained from cartilage indentation. Yellow line plots the load response of the cartilage to the indenter dis- placement (displayed in blue line) of fifty micron from the cartilage surface. 15	15
2.6 Different type of curve-fits. (A) Ramp displacement curvefit, (B) Total curvefit (ramp displacement together with holding, (C) Curvefit of relax- ation or holding portion . . . . .	16
2.7 Average r-square values for curve-fit of ramp, ramp with relaxation and relaxation portion. The 100 % goodness of fit line is shown in orange. . . . 17	17
2.8 Repeatability in measuring $E_1$ , $E_2$ , and $\eta$ from curve-fitting ramp, ramp along with relaxation and relaxation portions of the data. The yellow horizontal line is the line of no-change, bars close to this line with low standard deviation would mean minimum error in measurement. The cartilage was indented a total of six times. The bars show the normalized average of the results obtained from indents four to six, w.r.t. indents one to three. . . . .	18
2.9 Normalized peak load of subsequent indentations for different indenter sizes. Value of one (denoted by orange line) represents no-change. . . . .	19
2.10 Normalized values of (A) Spring 1 stiffness, (B) Spring 2 stiffness, and (C) Dashpot constant, for different indentation depths. . . . .	21
2.11 Values of peak load obtained at indentation sets two and three were nor- malized by the first set. (A) without protease inhibitors (B) with protease inhibitors . . . . .	23



Figure	Page
2.12 Five indentation points . . . . .	24
2.13 Values of peak load at every set of indentation were divided by the first set to get normalized values. Orange line indicates no-change with respect to first indentation set. . . . .	25
3.1 Control and Crosslink specimen submerged in protease solution in PBS before treatment . . . . .	28
3.2 Crosslink sample immersed in CASPc solution vs control sample immersed in PBS solution . . . . .	28
3.3 Depression in the center of laser profile . . . . .	29
3.4 Laser Profile before additional fiber. . . . .	30
3.5 Laser Profile after additional fiber. . . . .	30
3.6 Peak-Load over time. Five bars denote normalized value of peak load of the indents. Solid orange line shows the line of no-change in peak load as measured in subsequent indentations. . . . .	31
3.7 Peak-Load over time, after maintaining the fluid bath level. Five bars denote normalized value of peak load of indents. Solid orange line shows the line of no-change in peak load as measured in subsequent indentations. . . . .	32
3.8 Normalized values of no-CASPc control, CASPc control and crosslinked cartilage properties. Different groups of bars denote subsequent sets of indentations normalized with respect to first set. A: initial spring stiffness, B: Spring two stiffness, C: peak load, D: dashpot constant, E: equilibrium stiffness, F: time constant . . . . .	34
3.9 Normalized values of SLS parameters for 20 sec, 30 sec and 40 sec laser exposure. Different groups of bars denote subsequent sets of indentations normalized with respect to first set. A: initial spring stiffness, B: Spring two stiffness, C: peak load, D: dahpot constant, E: equilibrium stiffness, F: time constant . . . . .	36

## SYMBOLS

$\eta$	dashpot constant
$\tau$	time constant
$E_1$	initial stiffness / stiffness of spring 1 in SLS model
$E_2$	stiffness of spring 2 in SLS model
$E_{inf}$	equilibrium stiffness
$R$	radius of indenter
$h$	indenter displacement
$h_0$	maximum indenter displacement
$t_R$	time corresponding to maximum indenter displacement

## ABBREVIATIONS

OA	osteoarthritis
PTOA	post traumatic osteoarthritis
ECM	extra-cellular matrix
GAGs	glycoaminoglycans
AGEs	advanced glycation end products
PBS	phosphate buffer saline
CASPe	chloroaluminum sulfonated phthalocyanine
SLS	standard linear solid model
OCT	optimum cutting temperature
gm	gram
g-f	gram-force
Hz	hertz

## ABSTRACT

Chandwadkar, Shaunak A. M.S.M.E., Purdue University, December 2017. Indentation Protocol to Determine Viscoelastic Properties of Cartilage Before and After Crosslinking. Major Professor: Diane R. Wagner.

Osteoarthritis affects millions of people of different age groups around the world. With very few treatment options and the highly restricted capacity of cartilage to repair, new treatment options are needed. The objective of this thesis was to develop a repeatable cartilage testing protocol, which could be used to test cartilage properties and determine if crosslinking can be used as a potential treatment for osteoarthritis. Previous studies have shown CASPc can be used as a photo-sensitizer to obtain collagen crosslinking through a secondary process. The ability to perform cartilage crosslinking by light-activation, which could be done arthroscopically is especially attractive as this would allow the surgery to be minimally invasive.

The indentation protocol developed for a stress-relaxation test was able to achieve 95% repeatability, meaning the error in determining cartilage properties stayed within 5% of the average for tests performed at different times. Results of photo-chemical crosslinking demonstrated no change in cartilage stiffness when compared with control specimens. The spherical indenter chosen to indent the cartilage was suspected to apply less strain on cartilage as a result of its profile, which only compressed the cartilage instead of stretching its surface. The stiffness of CASPc control specimen was observed to be increasing when compared with no-CASPc control, as a result of added viscosity of CASPc solution. This elevated stiffness was observed to diminish over time due to the diffusion of CASPc from cartilage.

## 1. BACKGROUND

Articular cartilage is a soft load bearing tissue found in synovial joints. Its functions include providing low friction to facilitate joint movement and distributing loads and forces to bones during daily activities.

Osteoarthritis (OA) is a cartilage disease, which causes softening of cartilage tissue making it incapable of performing its basic functions efficiently. OA leads to severe joint pain and the inability to perform daily tasks such as walking or running [1]. OA affects a large portion of US population; more than 10 percent of US population was diagnosed with some form of arthritis during the year 2005 while in 2009, OA was the fourth most common cause of hospitalization, costing about \$ 40 billion in treatments [2] [3].

The post-traumatic osteoarthritis (PTOA) is a type of OA, which is due to acute damage to the cartilage. The damage might be caused by an external factor, such as car accidents and sports injuries, or other types of trauma.

Cartilage regeneration and repair practically stops after bones stop growing. Any damage to cartilage either by OA or PTOA is essentially permanent and might increase. Joint replacement surgery is highly invasive and not a permanent solution, in the sense that the artificial joint might need replacement over time. The basis of this research is to develop new treatment techniques for cartilage diseases [4].

## 1.1 Cartilage Structure and Composition

Cartilage is a highly resilient tissue made up specialized cells called chondrocytes while the cartilage extra cellular matrix (ECM) consists of water, proteoglycans and collagen along with other proteins in lesser amounts [5]. Cartilage is hydrated, with the water content varying between 70-80% by weight. The remainder is proteoglycans and type-II collagen. Proteoglycans are made up of a protein core which along with glycosaminoglycans (GAGs) forms tree-branch like structure. The proteoglycans bind with hyaluronic acid to form a proteoglycan aggregate which looks like several parallel linear branches, originating from a central stalk. Proteoglycans constitute approximately 30% of the dry weight of the articular cartilage [6].

Collagen is a type of protein fiber which comprises 60-70% of the dry weight of the tissue, and its density varies with the depth of the cartilage. To better understand the distribution of collagen we categorize the cartilage into zones: the superficial, the intermediate, the deep and the calcified cartilage zone (Fig. 1.1) [7].

The superficial layer provides a low friction surface to facilitate movement, has high collagen content with fibrils arranged parallel to the surface, while the proteoglycan content is low. The surface has less water content than the middle/intermediate zone. The superficial layer is the thinnest layer amongst the above-mentioned layers of cartilage. The chondrocytes are flattened and appear oval [6] [7].

The intermediate zone of the cartilage is less organized and contains a lower quantity of collagen than the superficial layer, and chondrocytes appear to be round. Proteoglycan content is higher than the superficial layer. This layer is thicker and contains a larger amount of water when compared to superficial layer of the cartilage.

The deep layer has fewer chondrocytes and lesser collagen content, with fibers perpendicular to the subchondral bone. Proteoglycan content is the highest amongst all the layers. The deep zone is the thickest layer of cartilage and highly organized with fibrils perpendicular to the subchondral bone.

The tidemark acts as a boundary between the deep and the calcified zone. The calcified zone contains a high level of calcium and hydroxyapatite which is responsible for binding the cartilage to the subchondral bone. The calcified zone transitions into subchondral bone with depth [6].

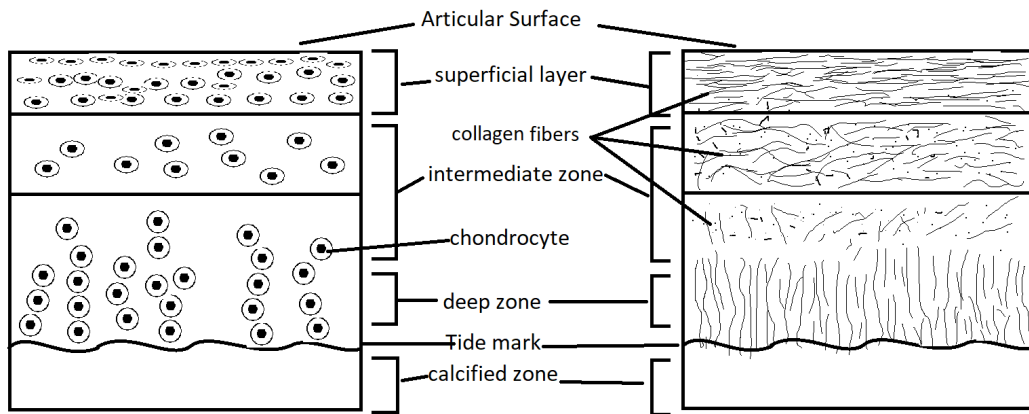


Fig. 1.1. Cartilage zones

## 1.2 Cartilage Disease

### 1.2.1 Osteoarthritis, OA

Osteoarthritis (OA) is a disease which results in the softening of the cartilage tissue. The softening of the cartilage eventually results in a reduction of the cartilage thickness. This phenomenon is due to the erosion of cartilage from the cartilage tissue surface.

Healthy cartilage tissue has very smooth surface and high load distributing properties. The erosion of the cartilage top surface makes it coarse and OA propagates through the depth of the cartilage, resulting in more cartilage loss and eventually the total loss of the cartilage layer over the subchondral bone. Tissue volume also decreases due to enzymes present in the cartilage [7].

Mechanical properties of cartilage are altered due to OA. The tissues load distributing property is reduced, and cartilage stiffness reduces. Swelling in cartilage tissue occurs due to loss of collagen fiber. This results in increased stress and pain in joints as the moves.

### 1.2.2 Post-Traumatic Osteoarthritis, PTOA

Another type of osteoarthritis, post traumatic osteoarthritis (PTOA) is cause by the wearing out of a joint that has been injured. The injury could be of varying types or varying reasons like a sports injury or car accident, etc. Such injuries can change the mechanics of the joint causing degradation of cartilage or quick wear out when compared to natural aging effects. PTOA accounts for 12 percent of total OA cases in the US, while more than 50 percent of individuals have a risk of developing PTOA after sustaining a knee or hip injury [8].

After the injury the cells die as necrosis occurs, and apoptosis causes more chondrocyte death [9] [10]. Due to cell death the cartilage thickness reduces as a result of degrading ECM and so does the tissue's capacity to perform normal operation.



According to an recent study glycosaminoglycans (GAGs) loss occurs after injury and is stress dependent. The study also showed that rate of cell death depend on the severity of trauma. [11].

PTOA changes the mechanical properties of cartilage, once ECM degradation is initiated, cartilage's load distribution capacity also reduces, and it cannot be restored. Cartilage thickness reduces, its load bearing capacity reduces and this is a painful phase for the individual [12] [13].

The damage to mechanical properties cannot be reversed and there are no current treatments for PTOA [14].

### **1.3 Cartilage Crosslinking**

Cartilage forms native crosslinks in the type II collagen, which improves the structural strength and stiffness of cartilage. The crosslinks are formed within and between different collagen molecules. The addition of exogenous crosslinks can enhance the cartilage ECM. The externally added crosslinks increase the strength of the cartilage tissue by strengthening the ECM and making it less susceptible to degradation [15].

#### **1.3.1 Photo-Chemical Crosslinking**

The process of forming chemical bonds with a light source to provide the required energy for photo-excitation of the crosslinking agent, and achieve crosslinking as a secondary process, is called photo-chemical crosslinking

Photo-chemical crosslinking can be broken down into three stages. In the first stage, a photosensitizer absorbs radiation and, as a result, forms an excited state. The second stage involves an internal reaction or excited stage within the photosensitizer. The third stage results into the formation of crosslinks from the products of stage two. [16] [17].

Photo chemical crosslinking can be achieved through a type-I process, where direct transfer of an electron or hydrogen atom occurs which produces radicals, or a type-II

process, where a direct interaction between the photo-sensitizer and oxygen molecule occurs to form a singlet oxygen by energy transfer [16]. The target molecule forms zero-length crosslinks within the polymers via a free singlet molecular oxygen ( $^1\text{O}_2$ ). One study showed that type-II crosslinking is necessary to form significant crosslinks in type-II collagen [18]. Chloroaluminum sulfonated phthalocyanine (CASPc) will be used as the photo-crosslinking sensitizer which, when exposed to 667 nm wavelength of light, results in the formation of singlet oxygen. As a secondary process singlet oxygen reacts with cartilage, and forms crosslinking of type-II collagen [17] [19]. CASPc is non-toxic even in high doses and its retention time is relatively short when injected in tissues [18].

The purpose of studying collagen crosslinking via photo-activation of CASPc was to investigate if it could be used to treat OA. The effects of this treatment were evaluated by performing indentation testing using a spherical indenter in a stress-relaxation protocol. The data obtained from indentation testing was fit to a mathematical model for viscoelastic material behavior.

Given the non-toxic nature of CASPc and the ability to localize the crosslinks by supplying the required light, only to the area where crosslinks are desired makes it medically feasible as an arthroscopic treatment that would be minimally invasive [18].

#### **1.4 Cartilage Indentation**

Indentation testing is a mechanical material testing method [20]. The spherical type of indenter was chosen for the experiment as it causes less damage to the cartilage compared to pyramid and other sharp indenter tips. A spherical indenter has been shown to create more centralized compression in the tissue and less stretching at the edges as compared to a flat indenter. Additionally the spherical indenter deforms a narrower and shallower region of the cartilage [21].

## 2. INDENTATION PROTOCOL

To obtain the cartilage properties, a micro-indentation method was used. Biomomentums Mach-1 Motion machine was used to perform the tests, with a load cell of range  $\pm 150$  gm. (AL312AL, Honeywell Industries Inc.). The load cell resolution was 0.0075 g-f while data was acquired at a rate of 100 Hz. The indentation protocol was developed for maximum repeatability and minimum variance. A stress-relaxation method was preferred versus creep loading due to its increased control. In order to detect the cartilage surface, a threshold value of 0.0875 g-f was set to trigger a function which would start the ramp displacement at the point of contact. Ramping or ramp displacement was linearly applied over time until the specified depth of indentation was reached. At the end of ramp loading, the displacement was held constant, and the relaxation period began.

Load versus time data during ramp loading and stress relaxation were used to find best-fit parameters of a standard linear solid (SLS) model for indentation of viscoelastic materials [22].

The cartilage samples were extracted from bovine stifles, obtained from a local butcher and stored frozen at  $-20$  ° C. After thawing overnight, the cartilage cubes were cut to roughly less than 1 cm in length, width and height from the femoral condyles on a band saw (MSKE, Skyfood equipment LLC.). To maintain the cartilage surface flat to the direction of indentation, the cubes were frozen on a freezing stage with an optimum cutting temperature (OCT) compound (Tissue Tek.) at  $-20$  ° C, with the cartilage surface facing downward. The subchondral bone was then milled flat on a milling machine (# 5000 Vertical milling machine, Sherline Products Inc.). At the end the samples were wrapped in gauze, vacuum sealed and stored frozen.

## 2.1 Standard Linear Solid Model of Indentation

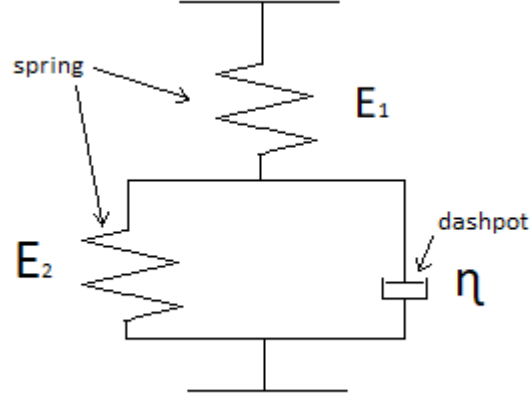


Fig. 2.1. Standard linear solid (SLS) model

The combined Maxwell and Kelvin-Voigt model for viscoelastic materials is shown in Fig. 2.1. For an arbitrary displacement, load as a function of time is defined by a linear viscoelastic Boltzmann integral for the spherical indenter [22].

$$F(t) = \frac{8\sqrt{R}}{3} \int_0^t G(t-u) \frac{dh^{\frac{3}{2}}}{du} u \, du \quad (2.1)$$

Where  $h$  is the displacement imparted by indenter tip,  $R$  is the indenter radius,  $u$  is the time variable and  $G(t)$  is the relaxation function for the material. The relaxation function  $G(t)$  for a SLS model is given by equation 2.2 [23] [1].

$$G(t) = \frac{E_1 E_2}{E_1 + E_2} + \frac{E_1^2}{E_1 + E_2} \exp\left(-\frac{(E_1 + E_2)t}{\eta}\right) \quad (2.2)$$

Where  $E_1$  is the stiffness of the first spring,  $E_2$  is the stiffness of the second spring in parallel with the dashpot, and  $\eta$  is the dashpot viscosity.

The indentation ramp loading and relaxation conditions are described as shown below [1].

$$h(t) = rt \text{ for } 0 \leq t \leq t_r \text{ (ramp displacement)} \quad (2.3)$$

$$h(t) = rt_R = h_0 \text{ for } t \geq t_R \text{ (relaxation or holding)} \quad (2.4)$$

Where  $r$  is the ramp velocity,  $t_R$  is the time required to reach peak displacement and  $h_0$  is the maximum displacement. Solving equation (2.1) using equation (2.2) and applying conditions from (2.3) & (2.4), the equation for the load-displacement as a function of time for the spherical indenter is.

$$F(t) = \left\{ \left[ \left( \frac{E_1 E_2}{E_1 + E_2} \right) H_{max}^{3/2} \left( 8 \frac{\sqrt{R}}{3} \right) \right] \right. \\ \left. * \left[ \left\langle \frac{E_1^2}{E_1 + E_2} \exp \left( - \frac{(E_1 + E_2) * t}{\eta} \right) \right\rangle \right] \right. \\ \left. * \left( \frac{\tau_1}{t_R} \right) \left[ \exp \left( \frac{t_r}{\tau_1} \right) - 1 \right] * H_{max}^{3/2} \left( 8 \frac{\sqrt{R}}{3} \right) \right] \right\} \quad (2.5)$$

Equilibrium stiffness is the stiffness of the model when it reaches equilibrium.

The Equilibrium stiffness  $E_{inf}$  was calculated as:

$$E_{inf} = \frac{E_1 * E_2}{E_1 + E_2} \quad (2.6)$$

The relaxation time constant  $\tau$  was calculated as,

$$\tau = \frac{\eta}{E_1 + E_2} \quad (2.7)$$

The value of parameters,  $E_1$ ,  $E_2$  and  $\eta$  that best fit the experimental data were found using the Matlab (Mathworks, Natrick, MA) optimization toolbox. The method of curvefit used was non-linear least square, in the Matlab function "FIT". The peak load,  $E_1$ ,  $E_2$ ,  $\eta$ , equilibrium stiffness  $E_{inf}$  and relaxation time constant  $\tau$  were reported.

## 2.2 Repeatability

Cartilage properties vary based on location, thickness, underlying bone, age of the donor, etc. Precautions were taken while handling the cartilage samples and performing experiment, so as not to damage the cartilage.

Repetitive testing with various testing parameters was performed to develop a protocol to achieve high repeatability. As performing crosslinking treatment required the specimen to be removed from the test setup and put back in for retesting, it was necessary that the indentation occurred at the exact same spot before and after crosslinking.

### 2.2.1 Ensuring Sample Repositionability

To ensure the cartilage samples stay firm on their respective locations on the test bed, superglue (Loctite Cyanoacrylate) was used to hold the samples in a 6-welled testing plate. About 1cm high cartilage cubes ensured substantial bone to be left under cartilage for securing it with glue, leaving the cartilage virtually untouched. The wells were then filled with phosphate buffer saline (PBS) to keep the cartilage hydrated to perform its function (Fig. 2.2).

The base plate which held the 6-welled plate and the cartilage samples inside it for indentation testing was machined with matching grooves. These grooves along with 4 securing bolts ensured no sliding movement between the 6-welled plate and the base plate, thus omitting any human error in the system.

The aluminum base plate was secured to the test bed of the Mach-1 Indentation testing machine with 2 M6 bolts.

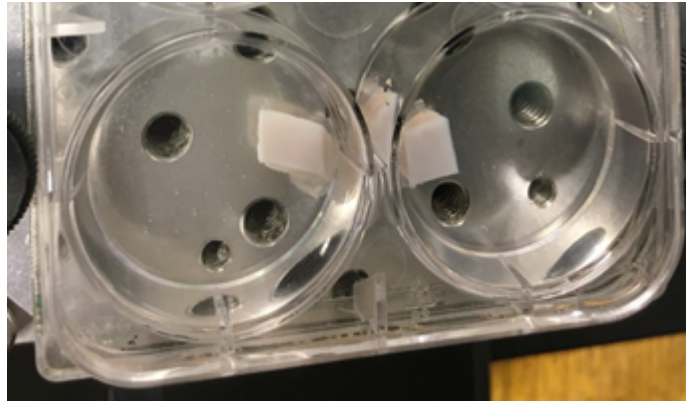


Fig. 2.2. Superglued cartilage specimen

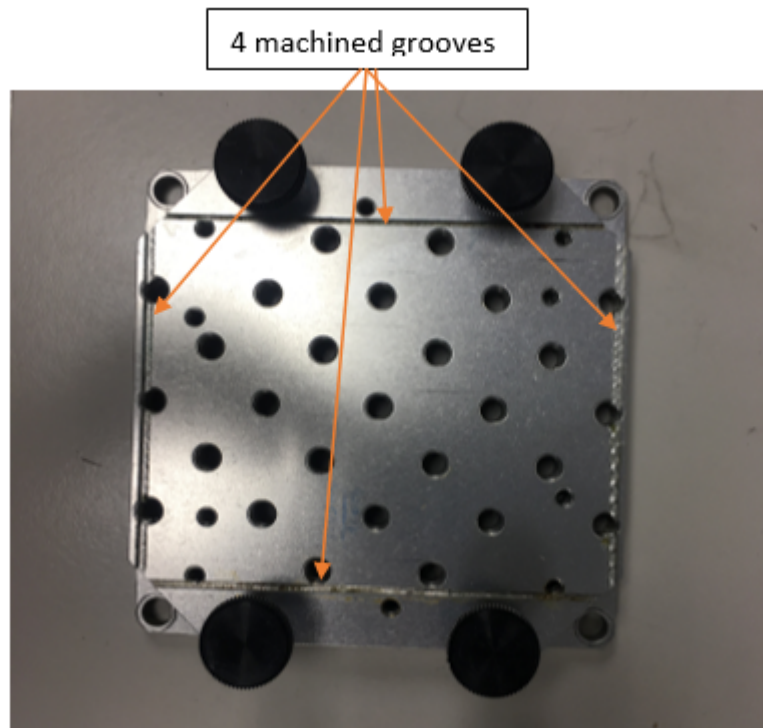


Fig. 2.3. Machined grooves on base plate

### 2.2.2 Actuator Calibration Protocol

A machine axis calibration protocol was developed to minimize any repeatability issue occurring due to machine error. The protocol required the machine to be calibrated to a known zero value in all three axes of movement. This calibration protocol would require measuring distances from the same origin on every axis.

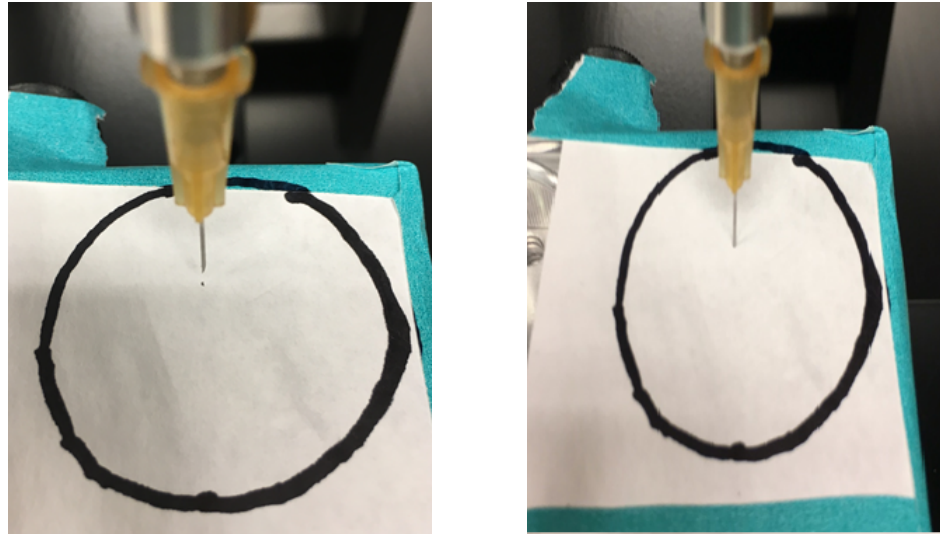
The left-most, the front-most and the top-most position of the linear actuators the indentation machine would be able to reach were selected as a starting point or the origin to calibrate the x, y and z axes respectively. The calibration for the axes was done before every single experiment and the repeatability was verified with a needle hole experiment.

To verify the repeatability the machine was booted up from off status and calibrated using the above protocol. A needle indenter was then used to poke a hole onto a paper stretched over the 6-welled plate (Fig 2.4 a, b). The coordinates where the needle punched a hole were read from the controller software and noted, and the machine was switched off, essentially resetting the calibration.

The base plate was then put back exactly as before using the same M6 bolts, followed by booting up the machine and re-calibration. The machine was made to indent at the previously obtained coordinates.

This experiment proved the high repeatability of the Mach-1 indentation machine to re-indent the same location. The needle entered inside the paper through the same hole which was previously poked by the needle.





(a) Needle punching hole in paper

(b) Needle entering previously punched hole

Fig. 2.4. Recalibration test, (a) shows the needle punching hole in a paper sheet (b) shows the needle entering the previously punched hole in paper after the machine was shut off and re-calibrated.

### 2.2.3 Indentation Data Interpretation

Several indentations were performed with the developed protocol as explained in previous sections. The data file consisted of time, x, y and z displacements as well as the load applied to the cartilage as a result of displacement.

The load vs time graph obtained from the data file is shown in Fig. 2.5. The load increases until the maximum displacement is reached, at this point the indenter does not move any further and instead stays at the same displacement value, exerting a load which is reduced over time due to the cartilages viscoelastic properties. This decrease in load is due to the PBS solution moving out of the cartilage through small pores.

This behavior is analogous to the mechanical model discussed in section 2.1 of this chapter. To further understand how the mechanical model is appropriate to represent cartilage behavior we can divide the obtained curve into two separate portions. One

being the ramp displacement portion, in which the displacement from zero to maximum is considered, and the other being the stress-relaxation or displacement holding portion in which the displacement remains constant although the load decreases as a function of time.

The above two cases can be implemented by the mathematical model.

Stage 1: The displacement applied from zero to maximum causes the load to rise until a peak value is reached. This similar displacement applied to the mechanical model would cause spring 1 to compress until the maximum displacement is achieved. The dashpot viscosity in this case plays a vital role in initially restricting the second spring from compressing. There was negligible displacement in dashpot during this stage.

Stage 2: As the displacement is held constant, the peak load is seen decreasing, the mechanical model explains this behavior with the simultaneous compression of dashpot and spring 2, whilst the spring 1 partially decompresses, and the model attains an equilibrium condition. With decrease in load being exponential, equilibrium would be attained at an infinite time point. The holding portion was set to hold the constant displacement for 20 seconds, and the calculated spring stiffnesss were used to determine the equilibrium stiffness of the model.

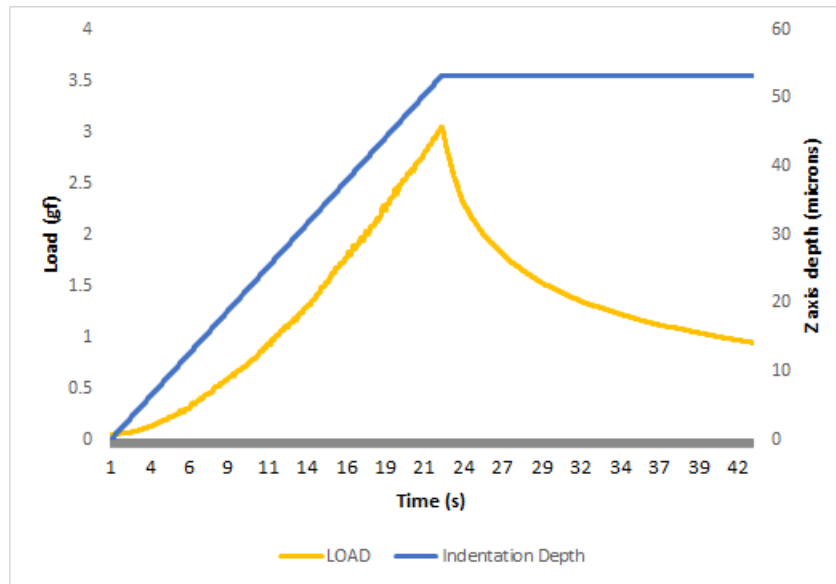


Fig. 2.5. Load and displacement versus time obtained from cartilage indentation. Yellow line plots the load response of the cartilage to the indenter displacement (displayed in blue line) of fifty micron from the cartilage surface.

### Curvefitting the Data

Curve fitting the obtained data to calculate the best-fit spring stiffnesses and dashpot constant was done using the optimization toolbox in Matlab (Mathworks, Natick, MA) using a non-linear least squares method. A test was performed on a cartilage sample, by indenting two points with each point indented six times. The mean values of indents four to six was normalized to the mean values of indents one to three. The indentation data was split into two sections namely before peak load (ramp displacement) and after peak load (holding) then curvefit was performed separately. Ramp displacement combined with holding was considered in a separate curvefit. The corresponding curve-fits are shown in Fig. 2.6 A, B & C.

The ramp displacement portion was initially fitted and the best-fit spring and dashpot constants were determined. Best-fit of ramp displacement (Fig. 2.6 A) showed that the model was not able to correctly fit the beginning couple of seconds of the data.

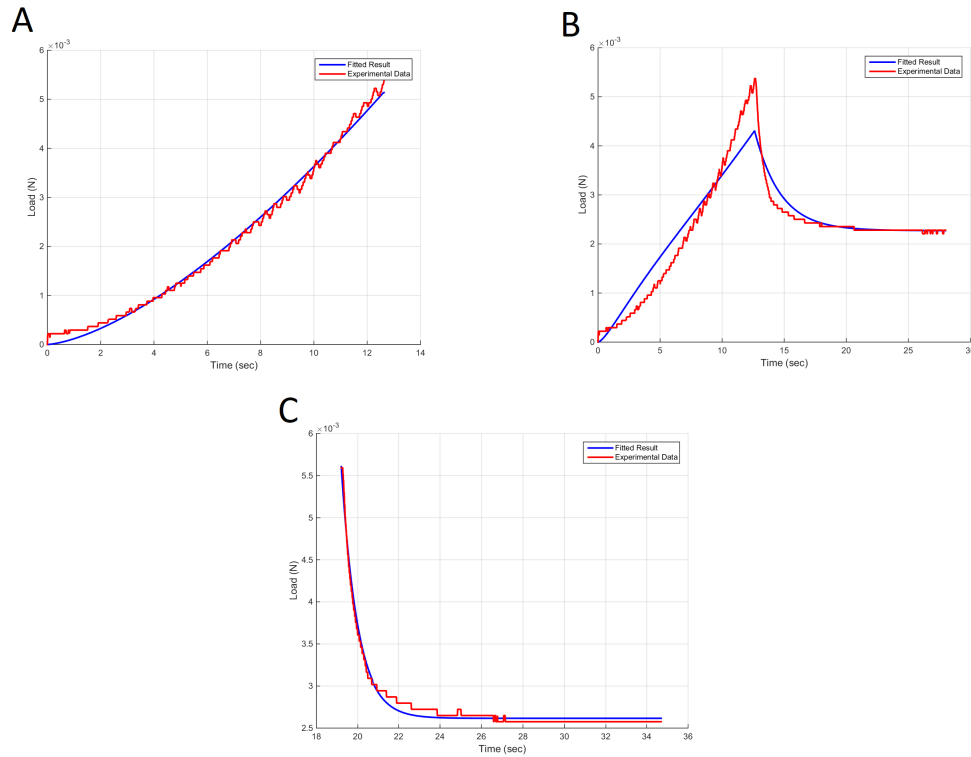


Fig. 2.6. Different type of curve-fits. (A) Ramp displacement curve-fit, (B) Total curvefit (ramp displacement together with holding, (C) Curvefit of relaxation or holding portion

Although the R-square value of best-fits for ramp displacement were about 98% (Fig. 2.7), the best-fit values of the dashpot constant were sometimes at the lower bound as set in the Matlab code, displaying high variation in the best-fit values (Fig 2.8). The contact conditions may have resulted in error in the measurement of load due to cartilage adhesion to the indenter.

The total data including the ramp displacement and the holding portion was also attempted to be curvefit. The accuracy of fit or the r-square value ranged between 80-90% which was lower by at least 10% than the individual curvefits to ramp displacement and the stress relaxation portions of the data. Therefore this curvefit was not considered.

The relaxation portion however proved to be ideal data to curvefit and determine the best-fit variables as the sensitivity of curvefit in the relaxation portion, to the contact conditions arising due to adhesion would be minimum because the relaxation portion starts when the indenter reaches 50 micron depth, from this point till the end of relaxation portion, the indenter displacement does not change.

The relaxation portion estimated the values of  $E_1$ ,  $E_2$  and  $\eta$  with accuracy of 10% of the average between different indents on the same cartilage sample at the same location, and the r-square value was between 97-99 %.

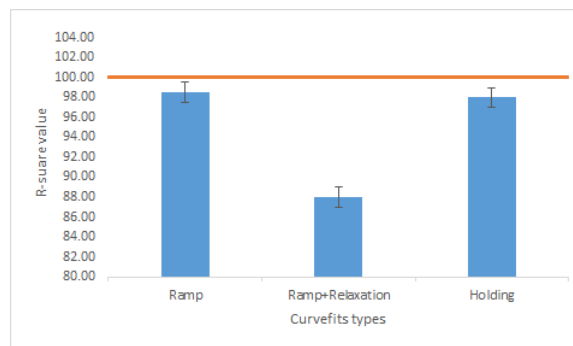


Fig. 2.7. Average r-square values for curve-fit of ramp, ramp with relaxation and relaxation portion. The 100 % goodness of fit line is shown in orange.

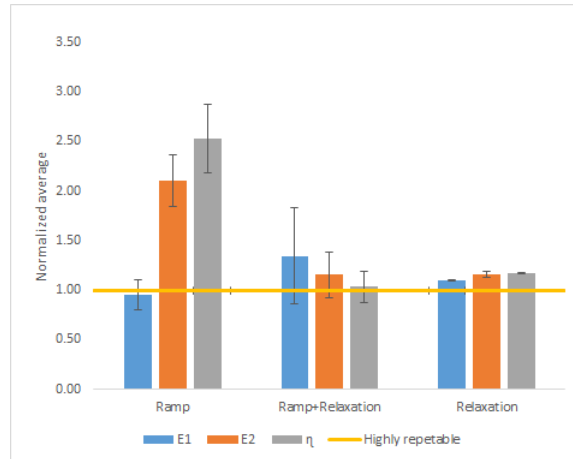


Fig. 2.8. Repeatability in measuring  $E_1$ ,  $E_2$ , and  $\eta$  from curve-fitting ramp, ramp along with relaxation and relaxation portions of the data. The yellow horizontal line is the line of no-change, bars close to this line with low standard deviation would mean minimum error in measurement. The cartilage was indented a total of six times. The bars show the normalized average of the results obtained from indents four to six, w.r.t. indents one to three.

#### 2.2.4 Indenter Size Optimization

Cartilage response is dependent on the type and size of indenter tip used. There are several factors which might affect the cartilage response to different size and shapes of the indenter. The area of the indenter which is in contact with the cartilage surface has a significant effect on repeatability and precise measurement of the properties.

A test was performed to evaluate the repeatability of the indenters with different sizes of spherical tip. Indenters with sphere diameters of 0.5mm, 1mm, 3mm, and 5mm were tested by indenting a cartilage sample at the same point six times, between each indent a waiting period of five minutes was introduced in order to allow the cartilage to equilibrate and return to its original state. A cartilage sample was indented at one location six times and the peak load obtained for indents two to six were normalized to the peak load from first indent.

A graph of the mean of normalized averages and standard deviation for different indenter sizes was plotted (Fig 2.9).

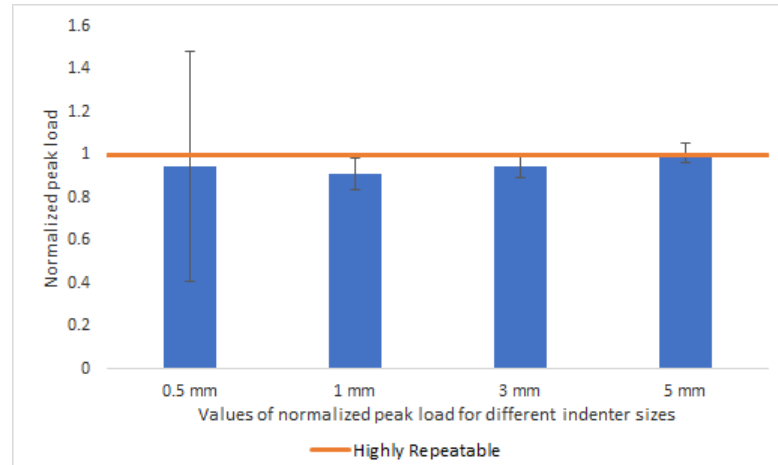


Fig. 2.9. Normalized peak load of subsequent indentations for different indenter sizes. Value of one (denoted by orange line) represents no-change.

As the graph shows, the 0.5 mm indenter was the least suited, as it had a standard deviation of about 45% of the average. The 1 mm indenter tip as well as the 3mm indenter tip were significantly better when compared to the 0.5 mm indenter with a standard deviation of about 10% of the average. The 5mm indenter was chosen for future indents given its high repeatability and low standard deviation of about 5% of the average in measuring the peak load with every indent.

### 2.2.5 Indentation Depth Optimization

The depth of indentation is basically the maximum displacement of the indenter measured from the cartilage surface. The depth of indentation was optimized because the surface of the cartilage has surface roughness, and lower depth of indentation would mean merely indenting the surface roughness, which could produce uneven results.

A cartilage specimen was indented to depths of 20,30,40 and 50 microns at five locations, and each location 4 times forming one set. The average of the data for  $E_1$ ,  $E_2$  &  $\eta$  from second set was then normalized to the first set of indentation and compared to determine the repeatability of each indentation depth.

Fig 2.10 displays the effect of indentation depths on the mechanical constants. Among the different indentation depths, 50 microns had a standard deviation that was under 5% of the average for all model constants, which was lower than the other depths. The indentation protocol was thus finalized to indent to a depth of 50 microns from the cartilage surface for further tests.



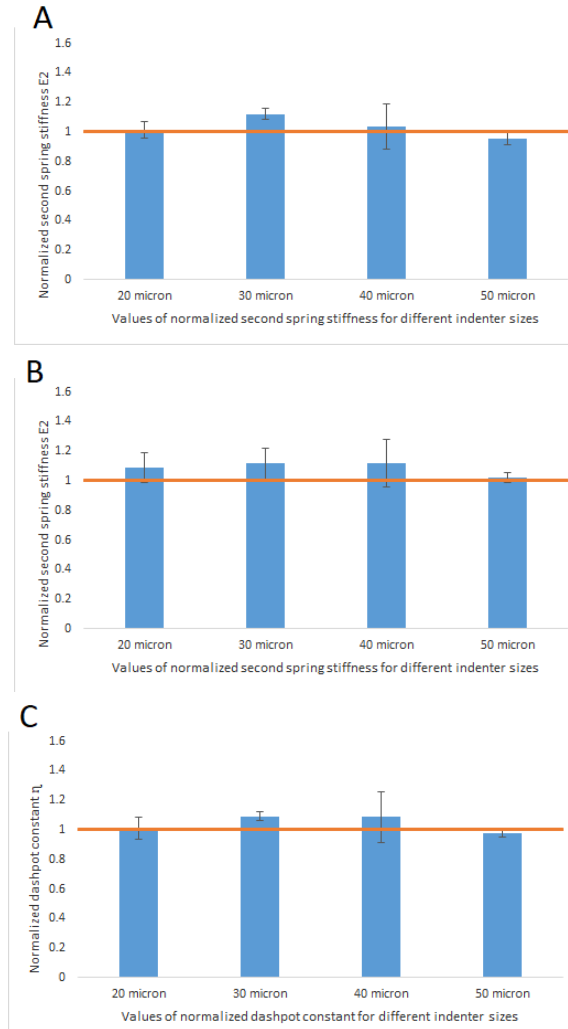


Fig. 2.10. Normalized values of (A) Spring 1 stiffness, (B) Spring 2 stiffness, and (C) Dashpot constant, for different indentation depths.

### 2.2.6 Cartilage Degradation and Arbitrary Error

A decreasing trend was observed with the protocol developed so far. A cartilage sample was indented in three indentation sets, indenting at five locations and each five locations were indented four times per set. The average value of peak load from second and third indentation sets was normalized to the average value from the first indentation set. The peak load decreased 7% over the span of three hours, suggesting the possibility of cartilage degradation (Fig 2.11 a). To stop the cartilage from degrading, protease inhibitors were added to PBS solution.

The concentration of protease inhibitors was 1mM ethylenediaminetetraacetic acid, 5 mM benzamidine and 10 mM n-ethylmaleimide [15].

Similar experiment as above was performed with the protease inhibitor solution to study whether cartilage degradation issue was solved.

The peak load from indentation sets two and three was normalized with respect to the first set, the data showed that the drop in peak load was reduced to about 1 % of the average (Fig. 2.11 B.). Additionally, it was decided to clean the indenter tip with iso-propyl alcohol between every experiment to rinse-off any residue left behind from indenting the cartilage.

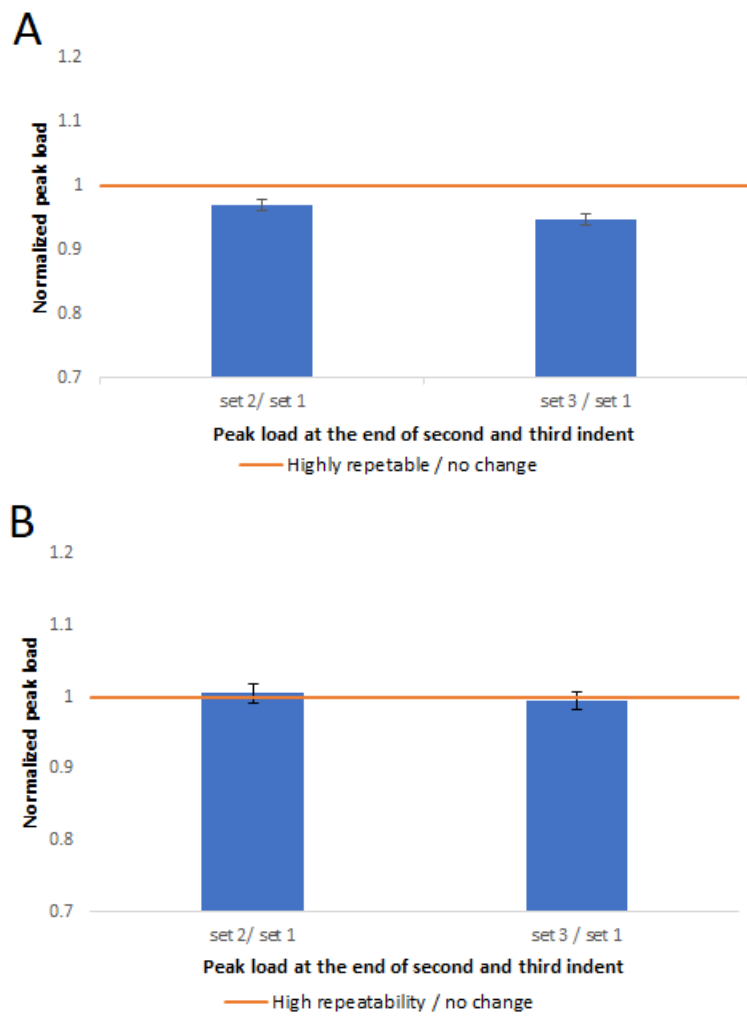


Fig. 2.11. Values of peak load obtained at indentation sets two and three were normalized by the first set. (A) without protease inhibitors (B) with protease inhibitors

### 2.2.7 Verification of Repeatability

The developed protocol was tested by repetitive indentation of cartilage specimens. The selection of points to indent was done with a simple rule of  $\pm 1$  mm in each direction from the center of the cartilage (Fig 2.12).

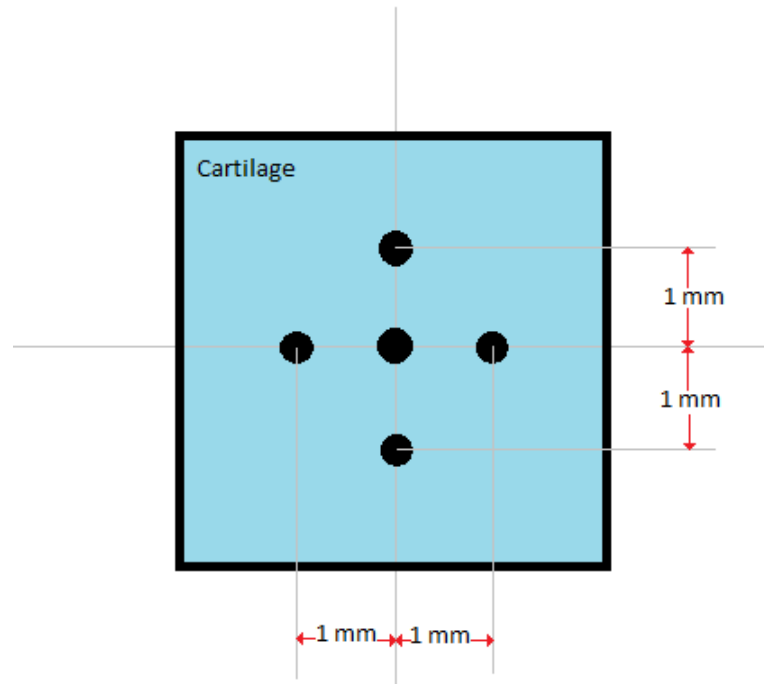


Fig. 2.12. Five indentation points

This method of selection five points to indent was used for all future indentations. The depth of indentation was set to 50 microns as it was proven to be optimum through previous experiments. At the same time the indenter used was a spherical 5 mm diameter tip. The time of holding was set to 20 seconds and for the sake of simplicity the ramping time was set to 20 seconds as well. To achieve the 20 seconds of ramp displacement time for 50 micron depth, the velocity of displacement was 2.5 microns/sec.

Five location on the cartilage were indented, each four times, which was considered one set of indent. Total of six such sets were performed and the average values from sets two through six were normalized with respect to the 1st set. Each indentation set required five hours to complete for total of 30 hours.

Results from the test showed a relatively steady peak load with six consecutive indents. This trend was consistent with other experiments. The average peak load of successive indents decreased by about 5% of the first one.

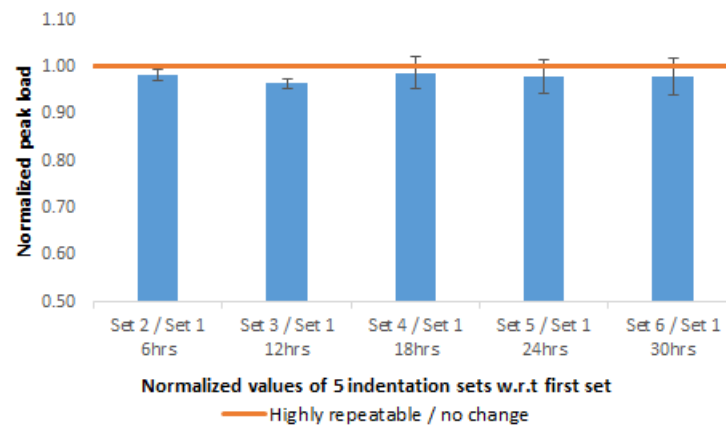


Fig. 2.13. Values of peak load at every set of indentation were divided by the first set to get normalized values. Orange line indicates no-change with respect to first indentation set.

### 2.3 Summary

The indentation protocol developed through different measures to achieve repeatability had the parameters shown in Table 2.1. Average values of properties from the curve-fit for untreated cartilage are found in Table 2.2.

Table 2.1.  
Indentation test parameters

Indentation depth	50 micron
Indenter size	$\phi$ 5 mm
Indentation velocity	2.5 micron/s
Cartilage bath	PBS+Protease inhibitors solution
Ramp/Relaxation time	20 sec. each
Curve-fitting region	Stress relaxation

Table 2.2.  
Untreated cartilage properties

Spring one constant, $E_1$	170 Mpascal
Spring two constant, $E_2$	6.24 Mpascal
Dashpot constant, $\eta$	988 Mpascal-Second
Peak load	9.995 g-f
Equilibrium stiffness, $E_{inf}$	5.86 Mpascal
Time constant, $\tau$	5.63 s

The protocol was repeatable to within 5% of the average of all viscoelastic model properties.

### 3. PHOTO-CHEMICAL CROSSLINKING

#### 3.1 Crosslinking Protocol

##### 3.1.1 Method

The protocol used for crosslinking was previously described [15]. Cartilage samples either acted as partially treated control specimen or underwent crosslinking treatment. The samples were indented at five different locations four times before any treatment for both control and crosslink specimens. At the end of the first indentation set, crosslinking was performed on the treated specimen while control specimen received partial crosslinking treatment. Indentation was performed again to compare the differences in properties of treated and partially-treated specimens.

Crosslinking was performed by subjecting the cartilage specimen to 15mM CASPc (Frontier Scientific) solution in PBS for 15 minutes. At the end of 15 minutes, the CASPc solution was drained and the cartilage specimen was covered with saran wrap to avoid dehydration. Specimens were then placed under 670 nm wavelength laser (BWTEK Inc, Newark, DE) for 30 seconds and the laser power was set to output at 1 mW [15] [17].

The partially treated control samples underwent similar treatment, except some did not receive the CASPc treatment and some were not exposed to laser. They will be referred to as (1) no-CASPc control; which did not receive CASPc solution but were exposed to laser. (2) CASPc control; which received CASPc solution but were not treated with the laser. After 30 seconds of laser exposure on both the control and crosslink specimen, the extra CASPc left behind was rinsed five times with PBS solution. Following the rinsing, five additional sets of indentation at each of the five points, were performed.

Each set of indentation took roughly four to six hours of time. Data interpretation was done as explained in Section 2.3

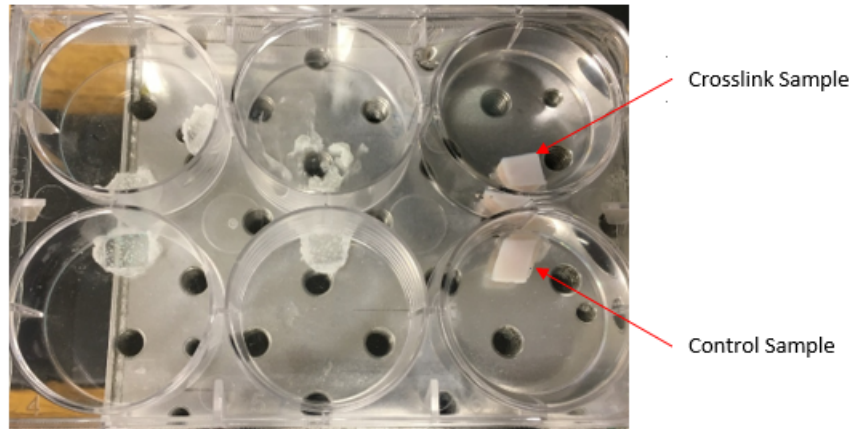


Fig. 3.1. Control and Crosslink specimen submerged in protease solution in PBS before treatment

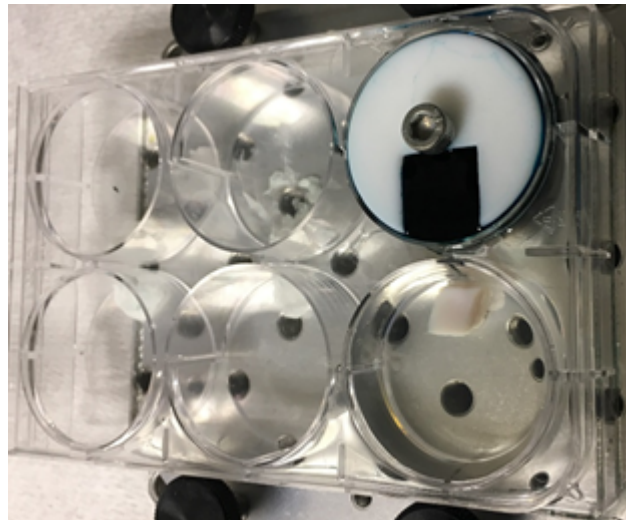


Fig. 3.2. Crosslink sample immersed in CASPc solution vs control sample immersed in PBS solution



### 3.1.2 Laser Output Issue

After careful inspection of laser power output, and laser profile, an issue with laser profile was detected. Shining the laser onto a flat surface from a distance revealed a depression in the center of the profile (Fig. 3.3).

To attend to this problem, initially cleaning the lasers fiber optic cable was done.

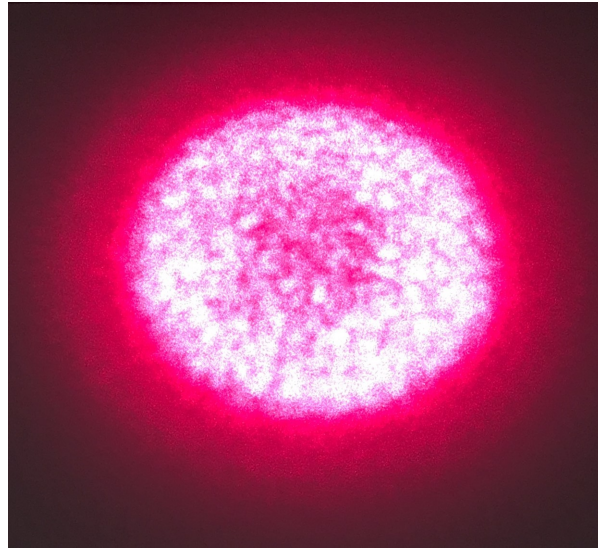
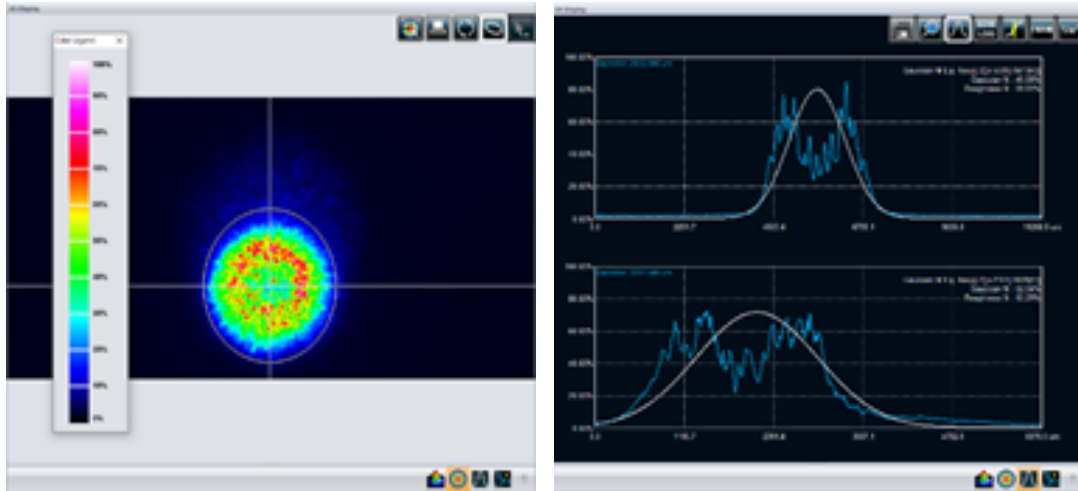


Fig. 3.3. Depression in the center of laser profile

The end of the fiber optic cable was cleaned with pressurized canned air, followed by iso-propyl alcohol. Cleaning seem to have no effect on the laser output profile. The solution to this was provided by the manufacturer and included the addition of a second fiber to the original fiber optic cable. To better understand the laser profile, the output was studied under an Optical Profiler (Edmund Optics, Beam Profiler #89-308). The studies comparing before and after addition of the second fiber suggested that the beam had become more uniform.

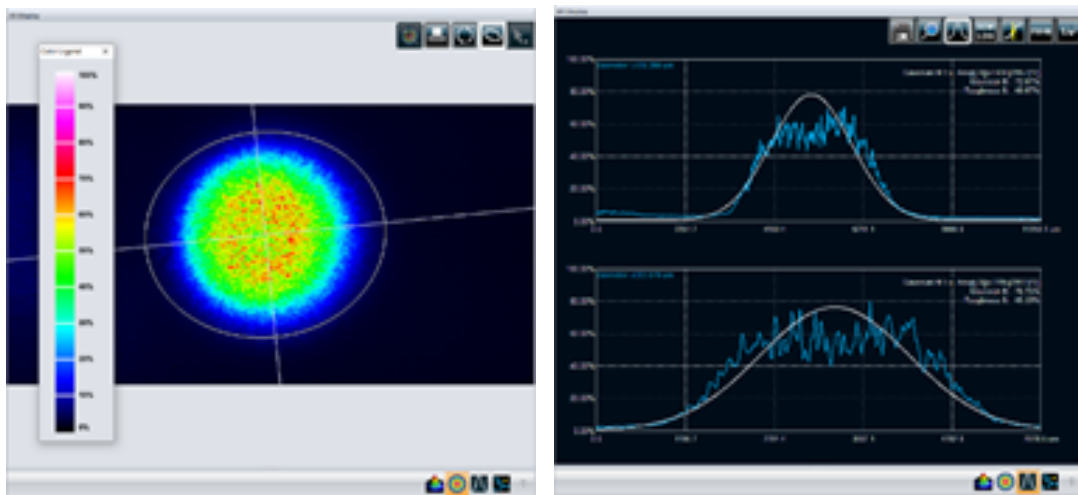
Fig. 3.4 a & b and Fig. 3.5 a & b compare the change in laser profile before and after the additional fiber. (a) shows the laser intensity profile, while (b) shows the Gaussian fit in x and y axis.



(a)

(b)

Fig. 3.4. Laser Profile before additional fiber.



(a)

(b)

Fig. 3.5. Laser Profile after additional fiber.

### 3.1.3 Stiffness Loss in Cartilage After Crosslinking

When evaluating the cartilage samples over time, loss of stiffness was observed. To evaluate the issue in depth, crosslinked cartilage was tested six times with each indent lasting roughly 5 hours.

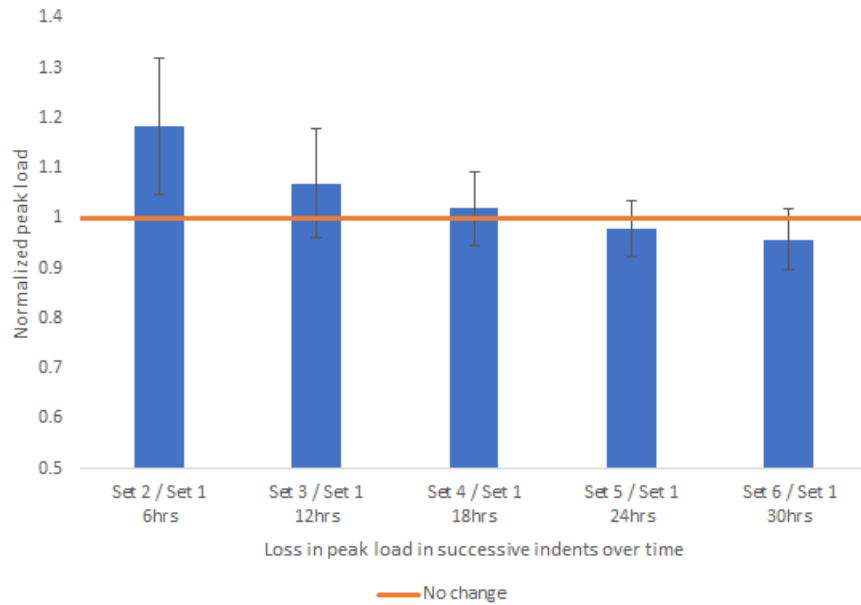


Fig. 3.6. Peak-Load over time. Five bars denote normalized value of peak load of the indents. Solid orange line shows the line of no-change in peak load as measured in subsequent indentations.

Fig. 3.6 shows combined data from five crosslinked specimens. The data suggests the loss of cartilage stiffness was about 25% of average over time. At the end of 30 hours of experimentation, significant evaporation of protease solution was observed. As the protease solution evaporates, the salts increased in concentration. This led to a phenomenon, in which the increased salt concentration decreased the osmotic pressure on the cartilage, forcing or facilitating higher flow rate of water through the cartilage. The increased flow-rate of water in the cartilage led to a loss of stiffness of the cartilage.

The solution to this issue was simple, and required replenishing the evaporated water with nano-pure water between every set of indentations.

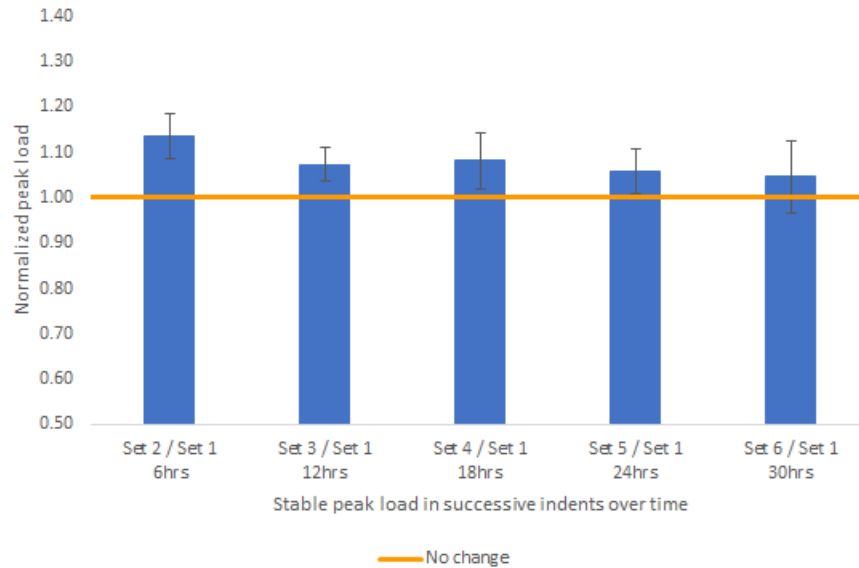


Fig. 3.7. Peak-Load over time, after maintaining the fluid bath level. Five bars denote normalized value of peak load of indents. Solid orange line shows the line of no-change in peak load as measured in subsequent indentations.

Fig. 3.7 shows combined data of 5 crosslinking specimens performed after replenishing the fluid level before every set of indentations. The results show the loss in stiffness reduced to 5% of average.

### 3.1.4 Indentation

A series of experiments with the indentation and crosslinking protocol were performed to determine if indentation could detect the change in cartilage stiffness due to crosslinking. Two types of controls were used along with a crosslinked sample to study the cartilage behavior in detail.

No-CASPc control specimens demonstrated the effects of the laser on a cartilage sample without the presence of the CASPc crosslinking agent.

The CASPc control specimens was immersed in CASPc, except no laser was shined on such control. CASPc control helped study the effect of CASPc on cartilage properties, as compared to the crosslinked cartilage.

The results obtained from no-CASPc and CASPc control specimens were compared with the crosslink specimens, which received both CASPc as well as laser treatment. In addition to laser exposure for 30 seconds, a study was performed in which the laser exposure time was changed to 20 and 40 seconds.

### 3.1.5 Effect of Photo-Chemical Crosslinking

In order to determine the effects of photo-chemical crosslinking on Articular cartilage, the changes in indentation properties before and after crosslinking, as well as on no-CASPc and CASPc controls were compared. The protocol as stated in Chapter 2, was used for indentation, and the crosslinking protocol as stated in the beginning of this chapter was used for crosslinking the specimen.

The specimen tested by performing six indentation sets, the normalized values of indentation sets two to six with respect to the first were evaluated. Fig 3.8 shows the comparison of viscoelastic properties of no-CASPc and CASPc control with crosslinked specimen, the normalized value of second set (immediately after treatment) and sixth set (30 hours after treatment) are shown.

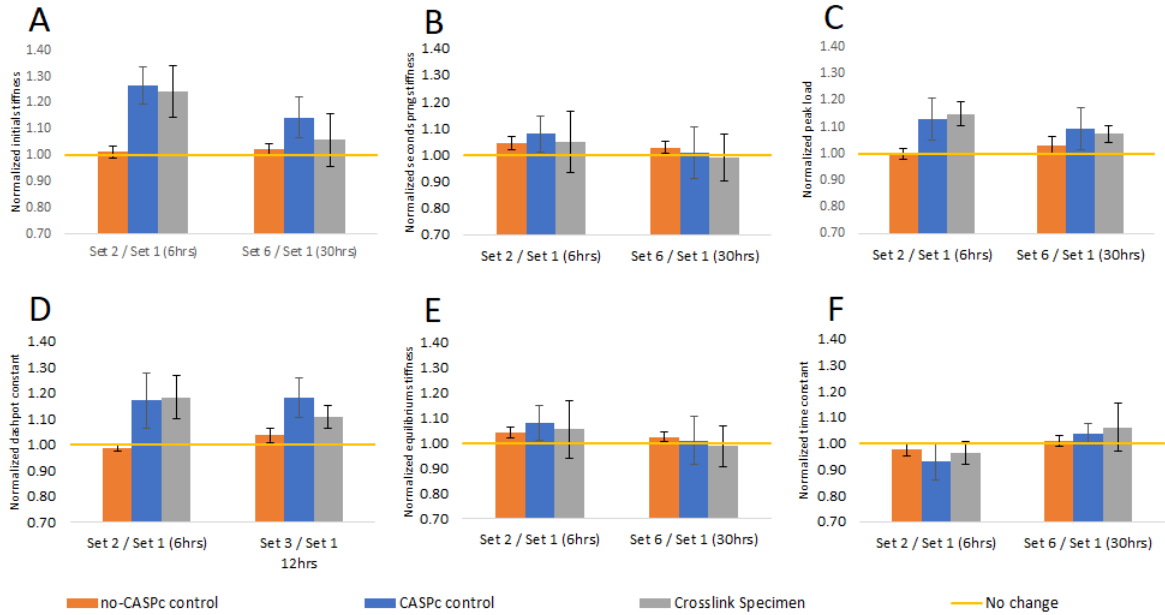


Fig. 3.8. Normalized values of no-CASPc control, CASPc control and crosslinked cartilage properties. Different groups of bars denote subsequent sets of indentations normalized with respect to first set. A: initial spring stiffness, B: Spring two stiffness, C: peak load, D: dashpot constant, E: equilibrium stiffness, F: time constant

The graphs show the change in the mechanical properties after crosslinking as compared to before crosslinking. After careful studying of the data, the following conclusions were made.

The results of no-CASPc control show that the experiment is highly repeatable with a small deviation in average. Dashpot constant  $\eta$  was observed to have maximum increase of  $4 \pm 9\%$ . The detected properties for no-CASPc control immediately after treatment were unchanged and 30 hours after treatment showed nominal changes.

1. As we compare the CASPc control and the crosslink specimen with respect to no-CASPc control, considerable and distinctive change in peak load, initial stiffness, and damping coefficient are observed immediately after the treatment. The difference seems to diminish over time. This phenomenon of increase in stiffness in CASPc

control along with crosslinked specimen, suggests that mere addition of CASPc to cartilage increases its stiffness. 15 mM CASPc solution in PBS was observed to be viscous, which might be one of the factor for initial rise in stiffness, as a viscous solution would take longer to diffuse from the cartilage, and would hinder the normal flow of water through the tissue.

2. As the exact depth of crosslinks formed due to exposure of laser is understudied, the developed indentation protocol is of 50 micron indentation depth is suspected to indent more of un-crosslinked tissue as the crosslinks formed are believed to be on the cartilage surface.

Additionally the spherical indenter was chosen because it compresses the surface roughnesses of the cartilage locally as opposed to flat-punch indenter. Although to detect the change in cartilage properties due to crosslinking, higher strain magnitudes would be better as it would stretch the cartilage surface where the crosslinking is likely to occur. In that case the flat-punch indenter would be better suited as it imparts greater strain at the articular surface than the spherical indenter [21].

3. The comparison of results of crosslinked specimen and CASPc control specimen led to the conclusion that indentation protocol developed was not sensitive to changes in stiffness due to crosslinking. The CASPc solution causes change in cartilage mechanical behavior in the crosslinked specimen. It would be necessary to diffuse all of the CASPc from the crosslinked sample to compare it with no-CASPc control for change in cartilage stiffness due to crosslinking. The CASPc control is better suited to compare change in cartilage stiffness due to crosslinking as the CASPc solution has similar effect on both CASPc control and crosslink specimen.

### 3.1.6 Laser Time Optimization

The indentation results with 30 seconds of laser exposure was indistinguishable from the CASPc control specimen, so to determine if different laser exposure time would attain higher amount of crosslinks formed, experimentation involving 20 and 40 seconds of laser exposure on cartilage with CASPc was performed. The purpose of evaluating two laser exposure times was to support the hypothesis that a different exposure time would result in higher amount of crosslinks formed and would in turn be detectable by the current indentation protocol.

The obtained data was also compared to 30 second crosslink samples.(Fig 3.9). No significant difference in properties was detected for any of the indentation taken after crosslinking.

However the  $\eta$  (damping coefficient) consistently displayed higher values in comparison with the no-CASPc control, which indicates the hydrating fluid was more viscous.

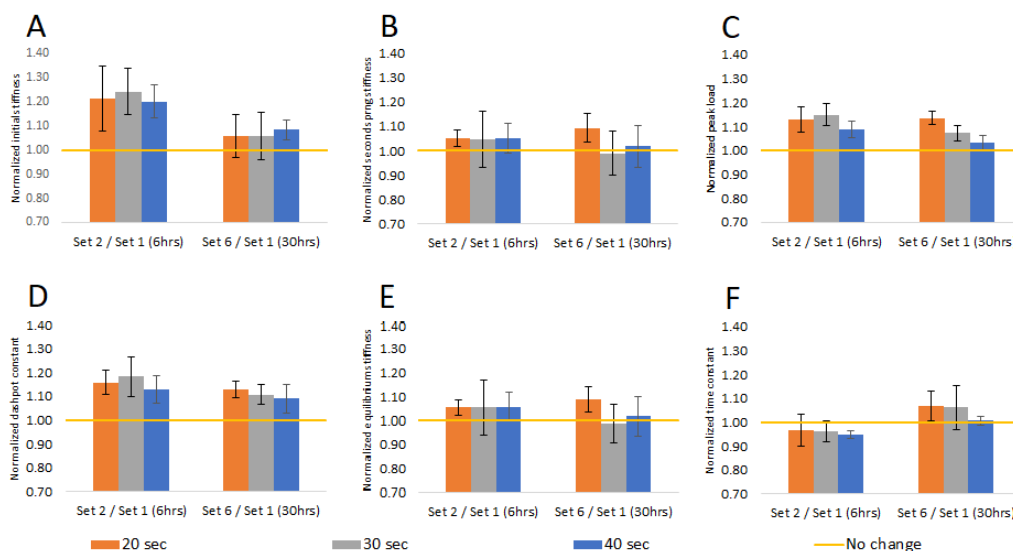


Fig. 3.9. Normalized values of SLS parameters for 20 sec, 30 sec and 40 sec laser exposure. Different groups of bars denote subsequent sets of indentations normalized with respect to first set. A: initial spring stiffness, B: Spring two stiffness, C: peak load, D: dahpot constant, E: equilibrium stiffness, F: time constant



## 3.2 Discussion

The crosslinking experiment examined the effect of photochemical crosslinking on bovine osteochondral cartilage specimen over the period a time to obtain increased in cartilage stiffness. Previous studies have shown that the increase in cartilage stiffness was observed with use of 15 mM CASPc in PBS for 15 min following laser treatment of 670 nm wavelength with 1mW power and 30 seconds of exposure [15].

The crosslink protocol used showed no increase in mechanical properties as compared to the CASPc control. However higher instantaneous stiffness and peak load (Fig. 3.8 A & C), higher dashpot constant (Fig. 3.8 D), were observed when compared with the no-CASPc control, while second spring stiffness (Fig 3.8 B), time constant(Fig 3.8 F) and Equilibrium stiffness (Fig 3.8 E) had no change.

The change in mechanical behavior after crosslinking and specified intervals of time showed a decreasing trend with each successive indentation set. The loss in cartilage stiffness may be a result of CASPc diffusion from the cartilage samples.

Another study was performed to determine if different laser exposure time would result into higher amount of crosslinking was performed with two additional laser exposure times of 20 sec and 40 sec. Comparison of the measured change in cartilage stiffness with this experiment showed there was no difference in mechanical properties with different laser exposure times (Fig 3.9). The results from comparison of controls along with the laser exposure time experiment, suggested an additional study would be necessary to optimize the indentation protocol for indentation depth, indenter size and indenter type, to detect the change in stiffness due to crosslinking. The spherical indenter compresses the cartilage more than imparting surface strain, on the other hand a flat-punch indenter would be better suited to detect and measure change in stiffness due to crosslinking at the articular surface, because it imparts more tensile strain on the cartilage surface [21].

Additionally as increase in stiffness was observed as a result of viscous CASPc solution (CASPc control specimen Fig 3.8) additional modifications to the crosslink protocol seem necessary to diffuse all the CASPc from the cartilage after crosslinking.

## 4. FUTURE DIRECTIONS

This thesis developed an indentation protocol for spherical indenter to repetitively test the cartilage for its viscoelastic properties. Studies were performed to evaluate the effect the CASPc as a crosslinking agent to elevate cartilage stiffness. The results show no change in cartilage stiffness after crosslinking as compared to CASPc control. Further studies and modification to the indentation protocol through experimentation would be necessary to develop cartilage crosslinking as a treatment for osteoarthritis.

### 4.1 Investigating Methods to Diffuse CASPc From Cartilage Tissue

The increase in cartilage stiffness in CASPc control (section 3.1.5) was due to slow diffuse of CASPc from the cartilage. Therefore additional study in determining ways to completely diffuse the CASPc from cartilage would prove beneficial for detecting distinguishable crosslink formation on the cartilage as compared to the no-CASPc control.

### 4.2 Optimize the Indentation Protocol

As discussed earlier the spherical indenter was suspected to compress the cartilage rather than stretching it, which means the spherical indenter applies less surface strain when compared to a flat indenter. The flat indenter may be better suited to detect the change in cartilage properties due to crosslinking as it induces more strain and stretches the cartilage surface more than the spherical indenter. Developing indentation protocol with a flat-punch indenter may be beneficial in detecting the change in cartilage properties due to crosslinking [21].

### **4.3 Detecting Crosslinks Through Alternative Mechanical Testing Methods**

While indentation was found to be highly repeatable in testing cartilage properties within 5% error, alternative method to detect change in cartilage properties would provide more insight. Impact testing and wear testing of cartilage would be beneficial to study as reaction to impact and wear resistance are important properties for cartilage to perform its normal function. Impact and wear testing would provide interesting insights about crosslinked cartilage's resistance to wear and impact.

## REFERENCES

## REFERENCES

- [1] M. E. McGann, C. M. Bonitsky, M. L. Jackson, T. C. Ovaert, S. B. Trippel, and D. R. Wagner, "Genipin crosslinking of cartilage enhances resistance to biochemical degradation and mechanical wear," *J Orthop Res*, no. 11, pp. 1571–9, 2015.
- [2] L. Murphy and C. G. Helmick, "The impact of osteoarthritis in the united states: A population-health perspective: A population-based review of the fourth most common cause of hospitalization in u.s. adults," *Orthopaedic Nursing*, vol. 31, no. 2, pp. 85–91, 2012.
- [3] R. Lawrence, C. Helmick, F. Arnett, R. Deyo, D. Felson, E. Giannini, S. Heyse, R. Hirsch, M. Hochberg, G. Hunder, M. Liang, S. Pillemer, V. Steen, and F. Wolfe, "Estimates of the prevalence of arthritis and selected musculoskeletal disorders in the united states," *Arthritis Care and Research*, vol. 41, no. 5, pp. 778–799, 5 1998.
- [4] K. M. Heinemeier, P. Schjerling, J. Heinemeier, M. B. Mller, M. R. Krogsgaard, T. Grum-Schwensen, M. M. Petersen, and M. Kjaer, "Radiocarbon dating reveals minimal collagen turnover in both healthy and osteoarthritic human cartilage," *Science Translational Medicine*, vol. 8, no. 346, pp. 346ra90–346ra90, 2016.
- [5] J. Mansour, *Biomechanics of cartilage*. Spain: Wolters Kluwer Health, 7 2013, pp. 69–83.
- [6] D. Lees and P. Partington, "Articular cartilage," *Orthopaedics and Trauma*, vol. 30, no. 3, pp. 265–272, 2016.
- [7] H. J. Mankin, V. C. Mow, J. A. Buckwalter, J. P. Ionnotti, and A. Ratcliffe, "Form and function of articular cartilage," *Orthopedic Basic Research*, pp. 1–44, 1994.
- [8] M. Stiebel, L. E. Miller, and J. E. Block, "Post-traumatic knee osteoarthritis in the young patient: therapeutic dilemmas and emerging technologies," *Open Access Journal of Sports Medicine*, vol. 5, pp. 73–79, 2014.
- [9] F. Heraud, A. Heraud, and M. Harmand, "Apoptosis in normal and osteoarthritic human articular cartilage," *Ann Rheum Dis*, vol. 59, no. 12, pp. 959–65, 2000.
- [10] A. Levin, N. Burton-Wurster, C. T. Chen, and G. Lust, "Intercellular signaling as a cause of cell death in cyclically impacted cartilage explants," *Osteoarthritis and Cartilage*, no. 8, pp. 702–711, 2001.
- [11] B. Mohanraj, G. R. Meloni, R. L. Mauck, and G. R. Dodge, "A high throughput model of post-traumatic osteoarthritis using engineered cartilage tissue analogs," *Osteoarthritis and cartilage / OARS, Osteoarthritis Research Society*, pp. 1282–1290, 2014.

- [12] R. U. Repo and J. B. Finlay, "Survival of articular cartilage after controlled impact," *J Bone Joint Surg Am*, vol. 59, no. 8, pp. 1068–76, 1977.
- [13] P. A. Kelly and J. J. O'Connor, "Transmission of rapidly applied loads through articular cartilage. part 2: Cracked cartilage," *Proc Inst Mech Eng H*, vol. 210, no. 1, pp. 39–49, 1996.
- [14] M. K. Lotz, "New developments in osteoarthritis: Posttraumatic osteoarthritis: pathogenesis and pharmacological treatment options," *Arthritis Research & Therapy*, no. 3, p. 211, 2010.
- [15] C. M. Bonitsky, "Wear and friction characteristics and crosslinked properties of gelatin and photochemical crosslinked articular cartilage," Thesis, 2015.
- [16] C. S. Foote, "Definition of type i and type ii photosensitized oxidation," *Photochemistry and Photobiology*, vol. 54, no. 5, pp. 659–659, 1991.
- [17] V. Sitterle, J. Nishimuta, and M. Levenston, "Photochemical approaches for bonding of cartilage tissues," *Osteoarthritis and Cartilage*, pp. 1649 – 1656, 2009.
- [18] E. Glassberg, L. Lewandowski, G. Lask, and J. Uitto, "Laser-induced photodynamic therapy with aluminum phthalocyanine tetrasulfonate as the photosensitizer: Differential phototoxicity in normal and malignant human cells in vitro," *Journal of Investigative Dermatology*, pp. 604 – 610, 1990.
- [19] H. Verweij, T. Dubbelman, and J. Van Steveninck, "Photodynamic protein cross-linking," *Biochimica et biophysica acta*, vol. 647, no. 1, p. 8794, 1981.
- [20] R. F. Bishop, R. Hill, and N. F. Mott, "The theory of indentation and hardness tests," *Proceedings of the Physical Society*, vol. 57, no. 3, p. 147, 1945.
- [21] W. C. Bae, C. W. Lewis, M. E. Levenston, and R. L. Sah, "Indentation testing of human articular cartilage: Effects of probe tip geometry and indentation depth on intra-tissue strain," *Journal of Biomechanics*, pp. 1039 – 1047, 2006.
- [22] L. Cheng, X. Xia, L. E. Scriven, and W. W. Gerberich, "Spherical-tip indentation of viscoelastic material," *Mechanics of Materials*, vol. 37, no. 1, pp. 213–226, 2005.
- [23] L. Cheng, X. Xia, W. Yu, L. E. Scriven, and W. W. Gerberich, "Flat-punch indentation of viscoelastic material," *Journal of Polymer Science Part B: Polymer Physics*, pp. 10–22, 2000.